10-1-2006

Structures and relative stability of neutral gold clusters: Au_n (n=15–19)

Satya S. Bulusu
University of Nebraska-Lincoln, sbulusu@iiti.ac.in

Xiao Cheng Zeng
University of Nebraska-Lincoln, xzeng1@unl.edu

Structures and relative stability of neutral gold clusters: Au$_n$ (n=15−19)

Satya Bulusu and X. C. Zeng[a)]

Department of Chemistry, University of Nebraska-Lincoln, Lincoln, Nebraska 68588 and Nebraska Center for Materials and Nanoscience, University of Nebraska-Lincoln, Lincoln, Nebraska 68588

We performed a global-minimum search for low-lying neutral clusters (Au$_n$) in the size range of $n=15-19$ by means of basin-hopping method coupled with density functional theory calculation. Leading candidates for the lowest-energy clusters are identified, including four for Au$_{15}$, two for Au$_{16}$, three for Au$_{17}$, five for Au$_{18}$, and one for Au$_{19}$. For Au$_{15}$ and Au$_{16}$ we find that the shell-like flat-cage structures dominate the population of low-lying clusters, while for Au$_{17}$ and Au$_{18}$ spherical-like hollow-cage structures dominate the low-lying population. The transition from flat-cage to hollow-cage structure is at Au$_{17}$ for neutral gold clusters, in contrast to the anion counterparts for which the structural transition is at Au$_{16}^-$ [S. Bulusu *et al.*, Proc. Natl. Acad. Sci. U.S.A. **103**, 8362 (2006)]. Moreover, the structural transition from hollow-cage to pyramidal structure occurs at Au$_{19}$. The lowest-energy hollow-cage structure of Au$_{17}$ (with C_{2v} point-group symmetry) shows distinct stability, either in neutral or in anionic form. The distinct stability of the hollow-cage Au$_{17}$ calls for the possibility of synthesizing highly stable core/shell bimetallic clusters M@Au$_{17}$ (M=group I metal elements). © *2006 American Institute of Physics*. [DOI: 10.1063/1.2352755]

INTRODUCTION

Gold clusters and nanoparticles hold great promise for applications in catalysis, medical sciences, and sensors.[1–5] Experimental and theoretical investigations have shown that gold clusters exhibit some unique properties such as strong relativistic effect and aurophilic attraction.[4] The strong relativistic effect coupled with the involvement of d orbitals leads to reduced $5d$-$6s$ energy gap as well as strong directional covalent bonds in gold clusters. As a result, gold clusters up to the size Au$_{20}$ have been shown to exhibit a variety of structures, including two-dimensional (2D) planar, shell-like "flat cage," spherical-like "hollow cage," and pyramidal.[6–18] In contrast, clusters of Cu and Ag only show planar and spherical-like compact structures in the same size range.[19–24] For neutral gold clusters, Au$_n$, previous high-level *ab initio* calculations show that a structural transition from 2D planar to three-dimensional (3D) structures occurs within the size range $n=8-10$.[13,14,17] For $n \geqslant 15$, Doye and Wales[25] performed the first global-minimum search of the lowest-energy clusters using Sutton-Chen potential of gold. They predicted that many low-lying neutral gold clusters favor compact structures. Another early study by Garzon and co-workers[26] showed that the low-lying neutral gold clusters with sizes $n=19$, 38, and 55 adopt amorphouslike compact structures. Note, however, that these early theoretical results were all based on empirical potentials of gold, in which the relativistic effect was not explicitly included.

Later, using a genetic-algorithm global optimization method coupled with tight-binding model and density-functional theory (DFT) total-energy calculation (considering relativistic effects), Wang *et al.*[7] found a shell-like flat-cage lowest-energy structure for $n=15$, and compact structures for $n=16-19$. The compact clusters typically consist of an inner core atom and outer "surface" atoms. In another DFT study[16] Fa *et al.* showed that the lowest-energy structure of $n=15$ exhibits shell-like flat-cage structure and that the low-lying structures of $n=16-19$ can be obtained by removing four, three, two, and one corner atoms of the pyramid Au$_{20}$,[10] respectively. After geometric reoptimization, the obtained clusters exhibit hollow-cage-like structures except $n=19$. We have recently carried out a joint experimental/theoretical study of anion gold clusters. We found that the predominant population of low-lying anion clusters for $n=16-18$ exhibits hollow-cage structures. The transition from the shell-like flat-cage to spherical-like hollow-cage structure occurs at $n=16$ for anion gold clusters. It is known that anion and neutral clusters often do not have the same lowest-energy structure, and thus do not show structural transition at the same size. For example, previous experimental/theoretical studies showed that the 2D-to-3D transition occurs at $n=12-13$ for anion clusters.[8,27] Olson *et al.*[13] used high-level *ab initio* coupled-cluster method to evaluate relative stability of 2D versus 3D low-lying neutral cluster of Au$_8$. It was found that 3D neutral clusters are lower in energy than the 2D neutral clusters. We also performed coupled-cluster calculation for low-lying clusters of Au$_9$ and Au$_{10}$ (Ref. 17) and found that 3D neutral clusters are lower in energy than the 2D neutral clusters, consistent with previous finding for Au$_8$.[13] The aim of this article is to search for candidates of the lowest-energy neutral clusters in the size range of $n=15-19$. We used the basin-hopping global optimization method[25,28] directly coupled with DFT total-energy calculation to generate a population of low-lying neutral clusters in the size range of $n=15-19$. We examined the cluster size at which the structural transition from the shell-like flat-cage to spherical-like hollow-cage structure occurs.
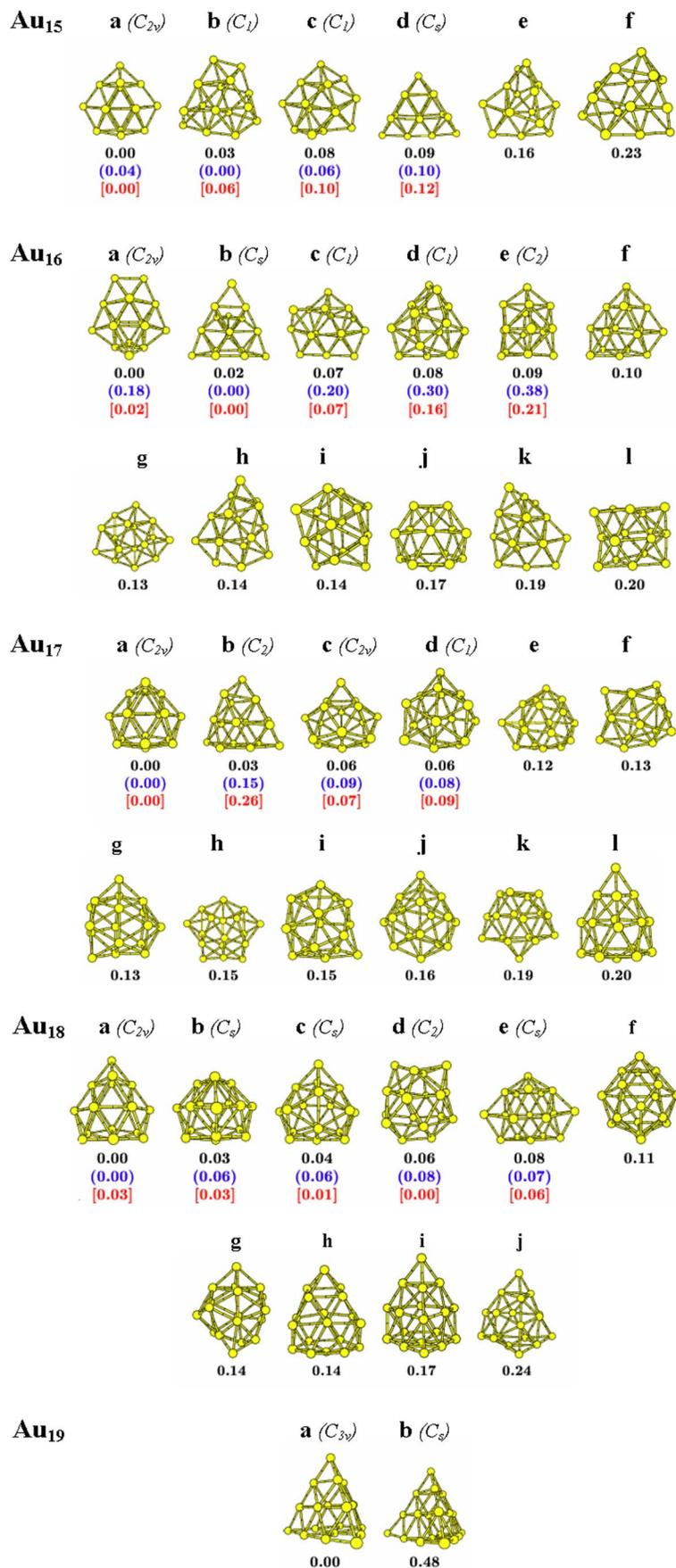
a)Electronic mail: xczeng@phase2.unl.edu

FIG. 1. (Color online) Structures of candidates for the lowest-energy cluster of $Au_{15}-Au_{19}$. The energy values (in eV) beneath each isomer are the relative energy with respect to the lowest-lying isomer calculated at the corresponding level of DFT. The energy values in *black color* are based on the PBE/DNP level of theory (Ref. 32). The energy values in *parentheses/blue color* are based on the PBEPBE/LANL2DZ level of theory (Ref. 33), while the energy values in *bracket/red color* are based on the single-point-energy calculation at the PBEPBE/SDD+Au(2f)//PBEPBE/LANL2DZ level of theory (Ref. 33).

TABLE I. Electronic energies (in a.u.) of the leading candidates for the lowest-energy neutral gold clusters ($Au_{15}-Au_{18}$) calculated at PBEPBE/ LANL2DZ and PBEPBE/SDD+Au($2f$) levels of theory. The boldfaced energy values highlight the lowest-energy isomers which can be dependent on the level of theory.

Cluster	PBEPBE/LANL2DZ// PBEPBE/LANL2DZ (in a.u.)	PBEPBE/SDD+Au($2f$)// PBEPBE/LANL2DZ (in a.u.)
15a	−2032.411 747 9	**−2037.287 282 1**
15b	**−2032.413 193 2**	−2037.284 952 9
15c	−2032.411 090 1	−2037.283 676 5
15d	−2032.409 599 7	−2037.282 931 6
16a	−2167.927 863 6	−2173.127 627 1
16b	**−2167.934 571 5**	**−2173.128 495 1**
16c	−2167.927 180 4	−2173.126 059 3
16d	−2167.923 540 7	−2173.122 581 5
16e	−2167.920 604 0	−2173.120 758 4
17a	**−2303.434 922 6**	**−2308.965 930 2**
17b	−2303.429 286 4	−2308.956 246 6
17c	−2303.431 659 1	−2308.963 530 4
17d	−2303.432 124 4	−2308.962 592 1
18a	**−2438.957 563 9**	−2444.812 152 3
18b	−2438.955 353 4	−2444.812 169 8
18c	−2438.955 376 9	−2444.813 004 0
18d	−2438.954 677 2	**−2444.813 306 2**
18e	−2438.955 167 9	−2444.811 147 0

Au$_{17a}$ **Au$_{17b}$**

FIG. 3. (Color online) A typical spherical-like hollow-cage structure (Au$_{17a}$) and shell-like flat-cage structure (Au$_{17b}$). A flat cage is defined such that besides the overall shape of the cluster is shell-like (or oblate in shape), the Au–Au lines (green lines) connecting through the central region of the cage (in the short-axis direction) are in the range of 3–4.5 Å. Thus, a flat cage may accommodate a small atom such as a hydrogen atom but cannot accommodate another gold atom without major structural distortion. A hollow cage is defined such that the Au–Au lines (green lines) connecting through the central region of the cage are all greater than 5.2 Å. Thus the hollow cage can accommodate another gold atom.

COMPUTATION METHODS

We performed a global-minimum search for the lowest-energy gold clusters in the size range of $n=15-19$. We employed the basin-hopping method coupled with (relativistic) density-functional theory calculation. This combined basin-hopping/DFT computational approach has been previously used to search for low-lying silicon clusters,[29] anionic gold clusters,[18] and bimetallic mixed clusters.[30]

In the basin-hopping search, we typically used 300–500 basin-hopping steps to generate at least 200 structurally different low-energy isomers for each size. We then identified those low-lying isomers whose energy value is within 0.2 eV from the lowest-lying isomer. These low-lying isomers are all regarded as candidates for the lowest-energy structure. This is because the DFT total-energy calculation entails certain intrinsic error bar for small-sized gold clusters.[13,14,17] We noticed that for topologically similar clusters, the error bar is relatively smaller, about 0.1 eV, whereas for topologically very different clusters, the error bar can be as large as a few tenths of eV.[13,17] In the DFT calculation, we employed the Perdew-Burke-Ezerhof (PBE) exchange-correlation functional[31] and double numerical polarized (DNP) basis set implemented in the DMOL3 code.[32] To examine basis-set effects on the relative energies, we further evaluated the relative energies among the low-lying isomers whose energy is within 0.1 eV from the lowest-lying one, by using a relativistic basis set (LANL2DZ) as well as a very large [SDD +Au($2f$)] basis set, respectively. The relative-energy values shown in parentheses and blue color (Fig. 1) are based on the optimization with the PBEPBE/LANL2DZ functional/basis set, while the relative-energy values shown in bracket and red color (Fig. 1) are based on the single-point-energy calculation at the PBEPBE/SDD+Au($2f$)‖PBEPBE/LANL2DZ level of theory, implemented in GAUSSIAN 03 software package.[33] Here "SDD+Au($2f$)" denotes the Stuttgart/ Dresden effective core pseudopotential (ECP) valence basis[34,35] augmented by two sets of f polarization functions
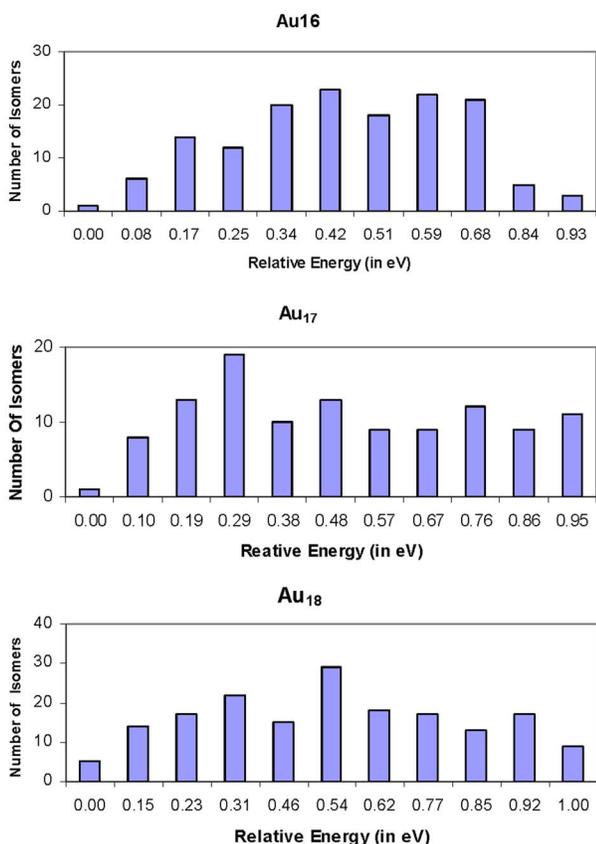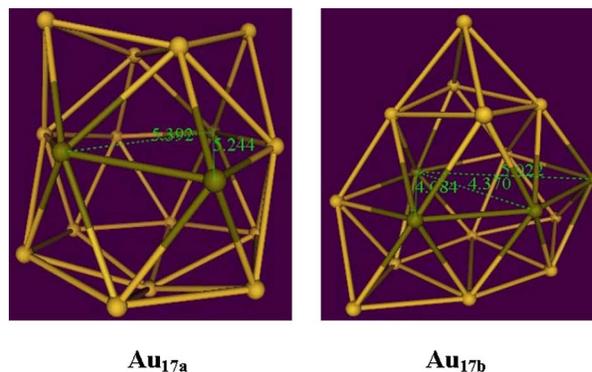

FIG. 2. (Color online) Histograms of the number of low-energy isomers vs the relative energies (with respect to the lowest-energy isomer calculated at the PBE/DNT level of theory) for Au$_{16}$, Au$_{17}$, and Au$_{18}$. The range of relative energy is set from 0 to 1 eV.

(exponents=1.425,0.468). Total energies are given in Table I.

RESULTS AND DISCUSSION

In Fig. 2, we show histograms of energy distribution for Au_{16}, Au_{17}, and Au_{18}. It can be seen that for Au_n ($n=16$–18), there are typically about 40–50 low-lying isomers whose energy is within 0.3 eV from the lowest-lying isomer. However, for Au_{19}, even the energy of the second lowest-lying isomer is already 0.48 eV higher than the lowest-lying isomer. Geometric structures of the low-lying isomers whose energy is within 0.2 eV from the lowest-lying isomer are plotted in Fig. 1. For the leading candidates whose energy is within 0.1 eV from the lowest-lying isomer, their relative energies calculated based on all three basis sets are displayed beneath each isomer (Fig. 1).

Among the low-lying clusters Au_n ($n=15$–18) displayed in Fig. 1, two generic cage structures can be identified: one is shell-like cage structure and another is spherical-like cage structure. Here we name the former *flat cage* and the latter *hollow cage*. Using Au_{17a} and Au_{17b} as an example (see Fig. 3), we define a flat cage (e.g., Au_{17b}) such that besides the overall shape of the cluster is shell like (or oblate in shape), the Au–Au lines (green lines in Fig. 3) connecting through the central region of the cage (in the short-axis direction) are within the range of 3–4.5 Å. Thus, a flat cage may accommodate a small atom such as a hydrogen atom but cannot accommodate another gold atom without major structural distortion. Moreover, we define a hollow cage (e.g., Au_{17a}) such that the Au–Au lines (green lines) connecting through the central region of the cage are all greater than 5.2 Å. Hence, the hollow cage can accommodate another gold atom.

Au_{15}. All the five leading candidates for lowest-energy isomers (Fig. 1) exhibit shell-like flat-cage structures. 15a can be viewed as being built upon the lowest-energy structure of Au_{14},[7,8,11,17,27] also a shell-like shaped isomer. Both 15a and the lowest-energy structure of Au_{14} possess C_{2v} symmetry. The energy ranking of the low-lying Au_{15} isomers is not very sensitive to the basis sets selected. As discussed above, because of the similarity in structures among these candidate low-lying clusters, we expect that the error bar in the DFT relative-energy calculation is relatively small, about the order of 0.1 eV. Hence, one of the 15a, 15b, and 15c isomers is likely the global minimum. 15a and 15b can be viewed as isoenergetic because their energy difference is less than 0.06 eV. As in the case of anion counterparts,[18] the flat-cage structures dominate the low-lying population of Au_{15}. It is worthy to note that 15a, 15b, and 15c are also among the top-five lowest-energy anion isomers of Au_{15}^- (Ref. 18).

Au_{16}. At $n=16$, the anion gold clusters undergo a transition from flat-cage to hollow-cage structure.[18] Indeed, a large population of low-lying anion isomers of Au_{16}^- exhibit hollow cages. In contrast, for neutral Au_{16}, the global-minimum search indicates that the flat-cage structures dominate the low-lying population, similar to the case of Au_{15}. The lowest-energy isomer 16a exhibits C_{2v} symmetry and is about 0.17 eV lower in energy than the T_d-symmetry hollow-cage 16j (Fig. 1). The latter is a leading candidate for the lowest-energy anion isomer of Au_{16}^- (Ref. 18). The second leading candidate for the lowest-energy Au_{16}, 16b, is merely 0.02 eV higher in energy than 16a at the PBE/DNP level and 0.02 eV lower at the higher level PBEPBE/SDD+Au(2f). Hence, based on DFT, 16a and 16b can be viewed as isoenergetic. Note that the geometry of 16b is sailing-boatlike, the only non-flat-cage isomer among 16a–16e (Fig. 1). Since the geometric structure of 16b is drastically different from other flat-cage isomers, high-level *ab initio* calculation is required to evaluate their relative stability. To this end, we performed single-point energy calculation of 16a and 16b using the resolution-of-the-identity coupled-cluster (RI-CC2) method with the TZVP basis set. The TURBOMOLE software program was used for this independent total-energy calculation.[36] It is found that the flat-cage structure 16a is 0.68 eV lower in energy than the boatlike structure 16b. This result shows that the global minimum of Au_{16} is most likely a flat-cage isomer. The two flat-cage isomer candidates, 16a and 16c, hold the highest possibility to be the global minimum, on the basis of DFT calculation with the large basis set (Table I).

Au_{17}. For neutral Au_{17}, the predominant population of low-lying isomers exhibits hollow-cage structures, as in the case of anion Au_{17}^- (Ref. 18). Therefore, we can conclude that, for neutral gold clusters, the structural transition from the shell-like flat-cage to spherical-like hollow-cage occurs at Au_{17}. Note that, for anion clusters, the transition is at Au_{16}^-. More interestingly, the geometric structure of the lowest-lying isomer 17a is identical to that of the lowest-energy isomer of Au_{17}^- (Ref. 18). In fact, DFT total-energy calculations with all three basis sets [DNP, LANL2DZ, and SDD+Au(2f)] give consistent prediction to the energy ranking (Fig. 1), that is, 17a is the lowest-energy isomer. It appears that 17a is distinctly stable. This distinct stability of 17a, either in neutral or in anionic form, is a unique case in the sense that for other gold clusters in the size range of n=15–18 the predicted lowest-energy isomer is always more or less sensitive to the selected basis set. 17a processes C_{2v} symmetry and can be viewed as placing one atom on the top of 16j (Fig. 1). The other two candidates for the lowest-energy isomer of Au_{17}, 17c and 17d, also exhibit hollow-cage structures. However, 17b exhibits a flat-cage structure with C_2 symmetry. DFT calculation with the larger basis set [SDD/Au(2f)] shows that 17b is about 0.26 eV higher in energy than 17a.

Au_{18}. For neutral Au_{18}, again, the hollow-cage structures dominate the population of low-lying isomers. As shown in Fig. 1, all top-five candidate lowest-energy isomers are within 0.08 eV in energy among each other. Because there exist a large number of nearly isoenergetic isomers for Au_{18}, it is not surprising that the energy ranking predicted is sensitive to the selected basis sets (as shown by the relative-energy values in black, blue and red in Fig. 1). Hence, DFT alone cannot determine the true global minimum of Au_{18}. We can only conclude that the global minimum is likely to be one of the top-five isomers shown in Fig. 1. Note that for anion Au_{18}^-, the pyramidal-like isomer 18i (Fig. 1) is also a

leading candidate for the lowest-energy isomer.[18] However, in neutral form, 18*i* is not competitive energetically compared to the hollow-cage isomers 18*a*–18*e*. 18*i* is about 0.17 eV higher in energy than 18*a* at the PBE/DNP level, 0.33 eV higher at the PBEPBE/SDD+Au(2*f*) level, and 0.62 eV higher at the RI-CC2/TZVP//PBE/DNP level. The latter relative-energy result clearly shows that the pyramidal-like structure is not energetically as favorable as the hollow-cage structures for Au_{18}.

Au_{19}. As in the case of anion clusters,[18] the structural transition from hollow cage to pyramid occurs at *n*=19 due to the overwhelming stability of pyramid Au_{20} (Ref. [10]). Only two low-lying isomers of Au_{19} are shown in Fig. [1], both exhibiting pyramidal-like structures. 19*a* corresponds to the removal of a corner atom from the pyramid Au_{20}, while 19*b*, the second lowest-energy isomer, corresponds to the removal of an atom from the edge of the pyramid Au_{20}. Since the perfect pyramid Au_{20} structure is highly stable (magic-number cluster), a little structural distortion can cause appreciable energy increase. Indeed, 19*b* is 0.48 eV higher in energy than 19*a*, even though both isomers can be derived by removing only one atom from the pyramid Au_{20}.

CONCLUSION

On the basis of a global-minimum search by means of combined basin-hopping/DFT method we obtained a large population of low-lying neutral gold clusters in the size range of *n*=15–18, from which we identified several leading candidates for the lowest-energy cluster, including four for Au_{15}, two for Au_{16}, three for Au_{17}, five for Au_{18}, and one for Au_{19}. For Au_{15} and Au_{16} it is found that the shell-like flat-cage clusters dominate the population of low-lying clusters, while for Au_{17} and Au_{18} hollow-cage clusters dominate the low-lying population. Hence, the transition from flat-cage to hollow-cage structure is likely to occur at Au_{17}. In contrast, for the anion counterparts, the structural transition occurs at Au_{16}^-. Similar to the anion clusters, the transition from hollow cage to pyramid occurs at Au_{19}. The pyramid Au_{19} (19*a*) is much lower in energy than other low-lying isomers, and thus may be also considered as a magic-number cluster. It is also worthy to mention that the hollow-cage structure 17*a* (with C_{2v} point-group symmetry) shows distinct stability, either in neutral or in anionic form, compared to other low-lying isomers. This is a unique case because for other size of clusters considered here (except 19*a*) the predicted lowest-energy structure is always more or less sensitive to the selected basis sets, but 17*a* is not. The distinct stability of the hollow-cage 17*a* calls for the possibility of synthesizing highly stable endohedral gold clusters M@Au_{17} where M, for example, can be metal elements in group I. As such, the bimetallic core/shell clusters are not only closed-shell clusters but also satisfy the 18-electron rule,[37] a key factor responsible to the high stability of known gold-based bimetallic clusters.[30,38–40]

ACKNOWLEDGMENTS

[1] R. L. Whetten, J. T. Khoury, M. M. Alvarez, S. Murthy, I. Vez-mar, Z. L. Wang, P. W. Stephens, C. L. Cleveland, W. D. Ludedtke, and U. Landman, Adv. Mater. (Weinheim, Ger.) **5**, 8 (1996).

[2] C. A. Mirkin, R. L. Letsinger, R. C. Mucic, and J. Storhoff, Nature (London) **382**, 607 (1996).

[3] A. P. Alivisatos, K. P. Johnsson, X. Peng, T. E. Wilson, C. J. Loweth, M. P. Bruchez, and P. G. Schultz, Nature (London) **382**, 609 (1996).

[4] P. Pyykkö, Angew. Chem., Int. Ed. **43**, 4412 (2004).

[5] P. Schwerdtfeger, Angew. Chem., Int. Ed. **42**, 1982 (2003).

[6] H. Häkkinen and U. Landman, Phys. Rev. B **62**, R2287 (2000).

[7] J. Wang, G. H. Wang, and J. Zhao, Phys. Rev. B **66**, 035418 (2002).

[8] H. Häkkinen, B. Yoon, U. Landman, X. Li, H.-J. Zhai, and L.-S. Wang, J. Phys. Chem. A **107**, 6168 (2003).

[9] H. M. Lee, M. Ge, B. R. Sahu, P. Tarakeshwar, and K. S. Kim, J. Phys. Chem. B **107**, 9994 (2003).

[10] J. Li, X. Li, H.-J. Zhai, and L.-S. Wang, Science **299**, 864 (2003).

[11] L. Xiao and L. Wang, Chem. Phys. Lett. **392**, 452 (2004).

[12] F. Remacle and E. S. Kryachko, J. Chem. Phys. **122**, 044304 (2005).

[13] R. M. Olson, S. Varganov, M. S. Gordon, H. Metiu, S. Chretien, P. Piecuch, K. Kowalski, S. A. Kucharski, and M. Musial, J. Am. Chem. Soc. **127**, 1049 (2005).

[14] Y.-K. Han, J. Chem. Phys. **124**, 024316 (2006).

[15] A. V. Walker, J. Chem. Phys. **122**, 94310 (2005).

[16] W. Fa, C. Luo, and J. Dong, Phys. Rev. B **72**, 205428 (2005).

[17] Y. Gao, S. Bulusu, N. Shao, and X. C. Zeng (unpublished).

[18] S. Bulusu, X. Li, L.-S. Wang, and X. C. Zeng, Proc. Natl. Acad. Sci. U.S.A. **103**, 8326 (2006).

[19] M. Kabir, A. Mookerjee, and A. K. Bhattacharya, Phys. Rev. A **69**, 043203 (2004).

[20] G. H. Guvelioglu, P. Ma, X. He, R. C. Forrey, and H. Cheng, Phys. Rev. Lett. **94**, 026103 (2005).

[21] M. Yang, K. A. Jackson, C. Koehler, Th. Frauenheim, and J. Jellinek, J. Chem. Phys. **124**, 024308 (2006).

[22] R. Fournier, J. Chem. Phys. **115**, 2165 (2001).

[23] J. Zhao, Y. Luo, and G. Wang, Eur. Phys. J. D **14**, 309 (2001).

[24] E. M. Fernández, J. M. Soler, I. L. Garzón, and L. C. Balbás, Phys. Rev. B **70**, 165403 (2004); E. M. Fernández, J. M. Soler, and L. C. Balbás, *ibid.* **73**, 235433 (2006).

[25] J. P. K. Doye and D. J. Wales, New J. Chem. 773 (1998).

[26] I. L. Garzón, K. Michaelian, M. R. Beltrán, A. Posada-Amarillas, P. Ordejón, E. Artacho, D. Sánchez-Portal, and J. M. Soler, Phys. Rev. Lett. **81**, 1600 (1998); K. Michaelian, N. Rendón, and I. L. Garzón, Phys. Rev. B **60**, 2000 (1999).

[27] F. Furche, R. Ahlrichs, P. Weis, C. Jacob, S. Glib, T. Bierweiler, and M. M. Kappes, J. Chem. Phys. **117**, 6982 (2002).

[28] D. J. Wales and H. A. Scheraga, Science **285**, 1368 (1999).

[29] S. Yoo and X. C. Zeng, Angew. Chem., Int. Ed. **44**, 1491 (2005).

[30] Y. Gao, S. Bulusu, and X. C. Zeng, J. Am. Chem. Soc. **127**, 15680 (2005).

[31] J. P. Perdew, K. Burke, and M. Ernzerhof, Phys. Rev. Lett. **77**, 3865 (1996).

[32] B. Delley, J. Chem. Phys. **92**, 508 (1990).

[33] M. J. Frisch, G. W. Trucks, H. B. Schlegel *et al.*, GAUSSIAN 03, Revision C.02, Gaussian, Inc., Pittsburgh, PA, 2003.

[34] M. Dolg, U. Wedig, H. Stoll, and H. Preuss, J. Chem. Phys. **86**, 866 (1987).

[35] P. Schwerdtfeger, M. Dolg, W. H. E. Schwarz, G. A. Bowmaker, and P. D. W. Boyd, J. Chem. Phys. **91**, 1762 (1989).

[36] R. Ahlrichs, M. Bär, H.-P. Baron *et al.*, TURBOMOLE V5-8-0.

[37] P. Pyykkö, J. Organomet. Chem. (to be published).

[38] P. Pyykkö and N. Runeberg, Angew. Chem., Int. Ed. **41**, 2174 (2002).

[39] X. Li, B. Kiran, J. Li, H. J. Zhai, and L.-S. Wang, Angew. Chem., Int. Ed. **41**, 4786 (2002).

[40] Y. Gao, S. Bulusu, and X. C. Zeng, ChemPhysChem (to be published).